Desalination and Water Treatment
www.deswater.com
doi: 10.1080/19443994.2013.827777

52 (2014) 7473–7483
December

Taylor & Francis
Taylor & Francis Group

Solving equations describing the steady-state model of MSF desalination process using Solver Optimization Tool of MATLAB software

Mongi Ben Ali*, Lakdar Kairouani

Université de Tunis El Manar, Ecole Nationale d'Ingénieurs de Tunis, 05/UR/11-14 Unité de Recherche Energétique et Environnement, Tunis Belvédère, BP 37, 1002, Tunisie
Tel. +216 98 823 114; email: mongibenali2000@yahoo.fr

Received 30 August 2012; Accepted 11 July 2013

ABSTRACT

This work presents an algorithm for solving the large system of non-linear equations describing the steady state model of the two main layouts for the MSF process (the multi-stage flashing with brine recirculation and the once-through multistage flash desalination (MSF-OT)). The model accounts for the geometry of the stage, the mechanism of heat transfer, and the variation of the thermophysical properties of various fluids with temperature and salinity. In addition, the overall heat transfer coefficient was evaluated at each stage using convective heat transfer coefficient for internal and external flows, tube thermal conductivity and fouling resistance. Furthermore, the model takes into consideration the dependence of thermodynamic losses on stream flow rate, temperature, and the brine salinity. The system of equations was solved through an iterative procedure by using Solver Optimization Tool of MATLAB software. For each stage, the developed model was then used for evaluating the temperatures of the brine, distillate and cooling brine, the flow rates of brine outlet, distillate production, and steam heating. Finally, the resolution method was validated against the simulation results reported in the literature and the actual plant data at MSF-OT installation in Doha, Kuwait. The agreement was found to be good.

Keywords: MSF-BR; MSF-OT; Steady-state modeling; System of non-linear equations; Fsolve

1. Introduction

Water plays a central and vital role in all aspects of life. It is especially important for agricultural and industrial development. Unfortunately, freshwater is not available everywhere in the world. Moreover, global water shortages will become so catastrophic over the next 25 years that two in three people on the planet will face regular depletion of water supplies [1]. As we find 97% of all water in oceans, industrial desalination of sea water is becoming, in some countries, the main source of freshwater. Indeed, large numbers of desalination plants have been installed in the world.

Multistage flash (MSF) desalination process (Figs. 1 and 2) is the largest sector in the desalination industry. It accounts for more than 40% of the entire desalination market [2], and therefore, in some

*Corresponding author.

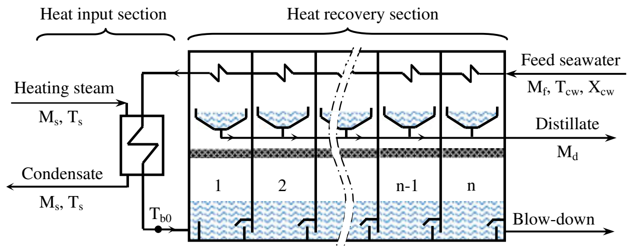

Fig. 1. Schema of once-through multistage flash desalination process (MSF-OT).

countries, it became the main source of freshwater for domestic, industrial, and agriculture consumption.

A lot of efforts have been made to enhance the operation of the MSF plants in the most efficient manner possible and therefore reduce the cost of water produced from such plants. Part of this is achieved by mathematical modeling which provides an inexpensive tool for finding the relationships among the various designs and operating parameters of the plants and therefore good understanding of the process.

Mathematical modeling of the MSF process is developed using the basic laws of thermodynamics [1–12]. Models can range from simple steady-state models with constant stream thermophysical properties [3,4,6,8] to rigorous models which consider properties' variations and losses [9–11]. The steady-state simulation of the MSF desalination process is based on the resolution of a large system of algebraic and nonlinear equations resulting from the mathematical modeling.

The main purpose of this paper is to present an algorithm for solving the system of equations describing a rigorous steady-state mathematical model for MSF-BR and MSF-OT desalination processes. The system will be solved through an iterative procedure by using the function fsolve of MATLAB software. The results will be checked and verified against actual plant data and previous simulation data given by Rosso et al. [3].

The next sections include a brief description of the MSF-OT process and the MSF-BR process, mathematical model and its solution, and finally comparison against actual and simulated data given in the literature.

2. Process description

There are two main layouts for the MSF process. The first is the once-through system (MSF-OT) and the second is the brine recirculation system (MSF-BR). The brine recirculation system is to be found on a larger scale than the once-through system [12]. Fig. 1 shows a schematic diagram for the MSF-OT process. As is shown, the system includes a number of flashing stages, and the brine heater. The flashing stage, shown in Fig. 3, consists of brine pool, vapor space, demister, condenser tubes, freshwater collecting tray, and inlet/outlet brine orifices. The intake sea water, M_f, passes through a series of heat exchangers; its temperature rises as it proceeds to the heat input section of the plant. Passing through the brine heater, the brine temperature is raised to its maximum value T_{b0} (also known as Top Brine Temperature, TBT). The brine then enters the first stage through an orifice thus reducing the pressure. As the brine was already at its saturation temperature for a higher pressure, it will become superheated and flashes to give off water vapor. This vapor passes through a wire demister to remove any entrained brine droplets, and on heat exchanger, where it releases its latent heat and condenses. The condensed vapor accumulates in the distillate tray located below the tube bundle. The process is then repeated all the way down the plant as both brine and distillate enter the next stage which is at a lower pressure.

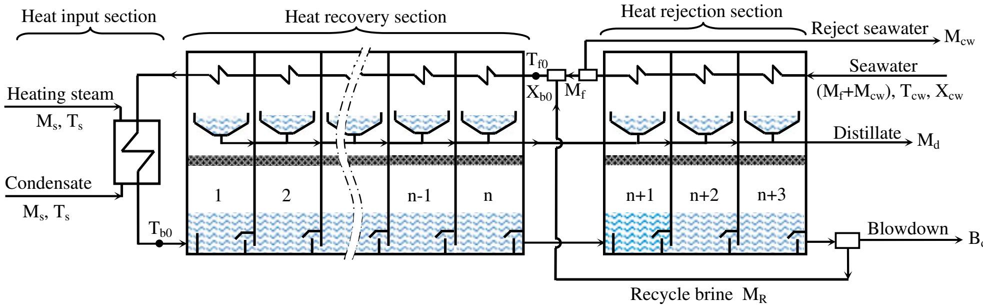

Fig. 2. Schema of brine recirculation multistage flash desalination process (MSF-BR).

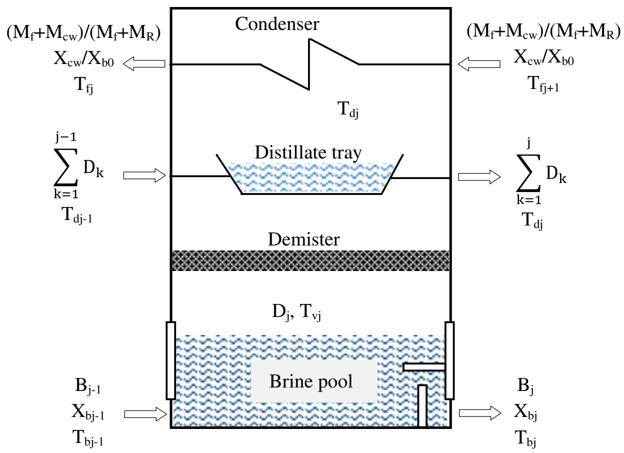

Fig. 3. Schema of the *j*-th stage of a MSF plant.

The brine recirculation system (MSF-BR) is shown in Fig. 2. As shown, the flashing stages are grouped in two sections, i.e. the heat recovery section and heat rejection section. The heat recovery section is identical to the flashing stages of the MSF-OT system. In the MSF-BR system, the feed to the plant, ($M_f + M_{cw}$), passes first through the heat rejection section which usually contains only two to three stages, and whose function is to reject the excess of heat added to the system in the brine heater and to cool the distillate product and the brine to the lowest possible temperature as they emerge from the last rejection stage. On leaving the first rejection stage, the feed stream is split into two parts, reject seawater M_{cw}, which passes back to the sea and a make-up stream M_f. Several pretreatments including deaeration, antifoam, and antiscalent additions must be applied to this stream before being combined with the recycle stream M_R. The combined stream, ($M_f + M_R$), now enters the heat recovery section, where it will undergo the same transformations described above in the case of the MSF-OT process. In the last stage of the plant, concentrated brine is partly discharged to the sea (B_d) and the remaining (M_R) is recycled as mentioned before.

3. Model equations

Many models have been developed to analyze the MSF water desalination process. All of these models are developed from the basic of mass balance, energy balance, and heat transfer equations. The system model can be simplified or made more complex depending on the assumptions used to define the heat transfer coefficient, thermodynamic losses, and physical properties. The mathematical model used in this work is given by Abdel-Jabbar et al. [4] and is supported by equations for calculating the thermal and physical properties of sea water, brine, and distillate water as function of temperature and salt concentration.

The assumptions used to develop the mathematical model are [4]:

- Steady state operation, which is the industry standard.
- The thermal and physical properties for feed sea water, brine, and distillate product are functions of temperature and salt concentration.
- The latent heat of formed/condensed vapur depends on temperature.
- The overall heat transfer coefficients in the condensers depend on the following parameters:

  (a) Flow rate of the condensing vapor.
  (b) Flow rate of the brine inside the condenser tubes.
  (c) Temperatures of the condensing vapor and the brine.
  (d) Physical proprieties of the condensing vapor and the brine, which includes thermal conductivity, viscosity, density, and specific heat.
  (e) The tube material, diameter, and wall thickness.
  (f) The fouling resistance.

- Thermodynamic losses include the boiling point elevation (BPE) and the nonequilibrium allowance (NEA).
- Distillate product is salt free.
- No subcooling of condensate leaving the brine heater.
- Heat losses to the surroundings are negligible.
- The effect of noncondensable gases on heat transfer is negligible.

The steady-state model equations are given in Fig. 4 and are constituted of a set of mass and energy balance equations that include the following:

- Material balance equation for each stage.
- Salt balance equation for each stage.
- Energy balance equations on flashing brine.
- Energy balance equations on feed sea water
- Flowing in condensers.
- Heat transfer equations.
- Brine heater model.
- Mixing and splitting equations.
- Overall material balance equations.

4. Thermophysical properties

The functions describing thermophysical proprieties of the streams of the plant are very

MSF-BR

Stage model (Figs. 2-3)

- Mass balance in the flash chamber : $B_{j-1} = B_j + D_j$
- Stage salt balance: $X_{bj-1}B_{j-1} = X_{bj}B_j$
- Energy balance for the flashing brine: $D_j\lambda_{vj} = B_{j-1}C_{pbj-1}(T_{bj-1} - T_{bj})$
- Energy balance for the condensers of the heat recovery section: $D_j\lambda_{cj}+C_{pdj-1}(T_{dj-1}-T_{dj})\sum_{k=1}^{j-1} D_k = (M_R+M_f)C_{pfj}(T_{fj}-T_{fj+1})$

  Where the vapor temperature above the demister is $T_{dj}=T_{vj}=T_{bj}-NEA_j-BPE_j$
- Energy balance for the condensers of the heat rejection section: $D_j\lambda_{cj}+C_{pdj-1}(T_{dj-1}-T_{dj})\sum_{k=1}^{j-1} D_k = (M_{cw}+M_f)C_{pfj}(T_{fj}-T_{fj+1})$
- Heat transfer equation for the condenser in the heat recovery section: $(M_R+M_f)C_{pfi}(T_{fi}-T_{fi+1})=U_{cj}A_c(LMTD)_{cj}$

  Where:
  - $(LMTD)_{cj}=(T_{fj}-T_{fj+1})/ln[(T_{dj}-T_{fj+1})/(T_{dj}-T_{fj})]$
  - The overall heat transfer coefficient (U_j) based on outer surface area of the tubes is evaluated using [6]

    $(1/U_j)=(d_o/d_i)(1/h_{ij})+(d_o/d_i)r_{fi}+(d_o/2k_{tube})ln(d_o/d_i)+(1/h_{oj})+r_{fo}$
  - The inside tube heat transfer coefficient h_i can be calculated from Dittus-Boelter equation [7]:

    $(h_id_i)/k_b=0.023Re^{0.8}Pr^{0.4}$
  - The condensation heat transfer coefficient h_o for the vapor side is [6]: $h_o = 0.725C_1\left[\frac{k_l^3\lambda_v\rho_l^2 g}{Nd_o\mu_l(T_d-T_{su})}\right]^{0.25}$
- Heat transfer equation for the condenser in the heat rejection section is : $(M_{cw}+M_f)C_{pfi}(T_{fi}-T_{fi+1})=U_{rj}A_{rj}(LMTD)_{rj}$

Brine heater model (Fig. 2)

- Energy balance equation: $M_s\lambda_s=(M_R+M_f)C_{ph}(T_{b0}-T_{f1})$
- Heat transfer equation: $M_s\lambda_s=U_hA_h(LMTD)_h$; where $(LMTD)_h=(T_{b0}-T_1)/ln[(T_s-T_1)/(T_s-T_{b0})]$

Blow-down splitter model (Fig.5)

- Mass balance: $B_{n+3}=B_d+M_R$

Makeup mixer model (Fig.6)

- Salt mass balance: $(M_R+M_f)X_{b0}=M_RX_{bn+3}+M_fX_{cw}$
- Energy balance: $(M_R+M_f)C_{pf0}T_{f0}=M_RC_{pbn+3}T_{bn+3}+M_fC_{pfn+1}T_{fn+1}$

Equations for the total plant (Fig.7)

- Overall mass balance: $M_f=M_d+B_d$ and $M_d = \sum_{j=1}^{n+3} D_j$
- Overall salt balance: $M_fX_{cw}=B_dX_{bn+3}$

MSF-OT

Stage model (Figs. 1-3)

- Mass balance in the flash chamber : $B_{j-1} = B_j + D_j$
- Stage salt balance: $X_{bj-1}B_{j-1} = X_{bj}B_j$
- Energy balance for the flashing brine: $D_j\lambda_{vj} = B_{j-1}C_{pbj-1}(T_{bj-1} - T_{bj})$
- Energy balance for the condensers: $D_j\lambda_{cj}+C_{pdj-1}(T_{dj-1}-T_{dj})\sum_{k=1}^{j-1} D_k = M_fC_{pfj}(T_{fj}-T_{fj+1})$
- Heat transfer equation for the condensers: $M_fC_{pfi}(T_{fi}-T_{fi+1})=U_{cj}A_c(LMTD)_{cj}$

Brine heater model (Fig. 1)

- Energy balance equation: $M_s\lambda_s=M_fC_{ph}(T_{b0}-T_{f1})$

Fig. 4. MSF process model.

complex and highly nonlinear. The relationships used in this work and shown in the following were reported by El-Dessoukey and Ettouney [5].

4.1. Sea water specific heat at constant pressure

$$C_p = (A + BT + CT^2 + DT^3) \times 10^{-3}$$

The variables A, B, C, and D are evaluated as a function of the water salinity as follows:

$$A = 4206.8 - 6.6197X + 1.2288 \times 10^{-2}X^2$$

$$B = -1.1262 + 5.4178 \times 10^{-2}X - 2.2719 \times 10^{-4}X^2$$

$$C = 1.2026 \times 10^{-2} - 5.3566 \times 10^{-4}X + 1.8909 \times 10^{-6}X^2$$

$$D = 6.8777 \times 10^{-7} + 1.517 \times 10^{-6}X - 4.4268 \times 10^{-9}X^2$$

where C_p in kJ/kg℃, T in ℃, and X is the water salinity in g/kg. The above correlation is valid over salinity and temperature ranges of $20{,}000 \leqslant X \leqslant 160{,}000$ ppm and $20 \leqslant T \leqslant 180$℃, respectively.

4.2. Sea water thermal conductivity

The sea water thermal conductivity is given by

$$\mathrm{Log}_{10}(k) = \mathrm{Log}_{10}(240 + AX) + 0.434\left(2.3 - \frac{343.5 + BX}{T + 273.15}\right) \times \left(1 - \frac{T + 273.15}{647.3 + CX}\right)^{1/3}$$

where k is the thermal conductivity in W/m℃, X is the salinity in g/kg, T is the temperature in ℃. The constants A, B, and C are equal to 2×10^{-4}, 3.7×10^{-2}, and 3×10^{-2}, respectively. The above correlation is valid over the following ranges, $0 \leqslant X \leqslant 160$ mg/kg and $20 \leqslant T \leqslant 180$℃.

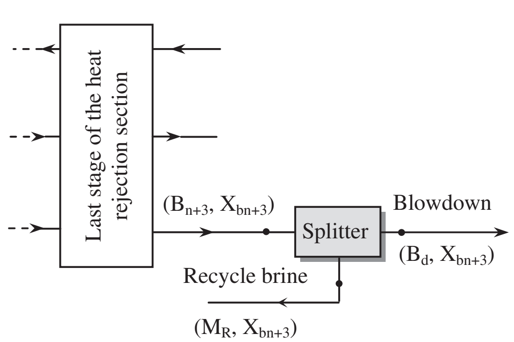

Fig. 5. Blow-down splitter.

4.3. Sea water dynamic viscosity

The correlation for the dynamic viscosity of sea water is given by

$$\mu = (\mu_w)(\mu_R) \times 10^{-3}$$

with

$$\mathrm{Ln}(\mu_W) = -3.79418 + 604.129/(139.18 + T)$$

$$\mu_R = 1 + AX + BX2$$

$$A = 1.474 \times 10^{-3} + 1.5 \times 10^{-5}T - 3.927 \times 10^{-8}T^2$$

$$B = 1.0734 \times 10^{-5} - 8.5 \times 10^{-8}T + 2.23 \times 10^{-10}T^2$$

where μ is the dynamic viscosity in kg/m.s, X is the salinity in g/kg, and T is the temperature in ℃. The above correlation is valid over the following ranges, $0 \leqslant X \leqslant 130$ mg/kg and $10 \leqslant T \leqslant 180$℃

4.4. Condensate density

The density correlation for the condensate which is considered as saturated liquid water is given by

$$\rho = 1/\left\{V_c\left(\frac{T_c}{T + 273.15} - 1\right)\exp\left(\sum_{i=1}^{6} f_i(T + 273.15)^{i-1}\right)\right\}$$

where $T_c = 647.286$ K, $V_c = 0.003172222$ m^3/kg and the values of f_i are given in the following

$f_1 = -2.781015567$; $f_2 = 0.002543267$; $f_3 = 9.845047 \times 10^{-6}$; $f_4 = 3.636115 \times 10^{-9}$; $f_5 = -5.358938 \times 10^{-11}$; $f_6 = 7.019341 \times 10^{-14}$.

In the above equation, ρ is in kg/m^3 and T is in ℃.

4.5. Enthalpy of saturated water vapor

The correlation for the water vapor enthalpy is given by

$$H = 2501.689845 + 1.806916015T + 5.087717 \times 10^{-4}T^2 - 1.122 \times 10^{-5}T^3$$

where T is the saturation temperature in ℃ and H is the vapor enthalpy in kJ/kg.

4.6. Latent heat of water evaporation

$$\lambda = 2501.897149 - 2.407064037T + 1.192217 \times 10^{-3}T^2$$

where λ in kJ/kg and T is the saturation temperature in °C.

4.7. Boiling point elevation

The correlation for the BPE of sea water is given by

$$\text{BPE} = AX + BX^2 + CX^3$$

with

$$A = (8.325 \times 10^{-2} + 1.883 \times 10^{-4}T + 4.02 \times 10^{-6}T^2)$$

$$B = (-7.625 \times 10^{-4} + 9.02 \times 10^{-5}T - 5.2 \times 10^{-7}T^2)$$

$$C = (1.522 \times 10^{-4} - 3 \times 10^{-6}T - 3 \times 10^{-8}T^2)$$

where T is the temperature in °C and X is the salt weight percentage. The above correlation is valid over the following ranges, $1 \leqslant X \leqslant 16\%$ and $10 \leqslant T \leqslant 180$°C.

4.8. Nonequilibrium allowance

The correlation for the NEA for the MSF system is given by

$$\text{NEA} = (\text{NEA}_{10}/(0.5\Delta T + \text{NEA}_{10}))^{0.3281L}(0.5\Delta T + \text{NEA}_{10})$$

with

$$\text{NEA}_{10} = (0.9784)^{Ti}(15.7378)^{H}(1.3777)^{Vb\times 10\text{-}6}$$

where T_i is the stage temperature in °C, H is the height of the brine pool in m, V_b is the brine flow rate per unit length of the chamber width in kg/(m.s), and ΔT is the stage temperature drop in °C.

5. Solution of the systems of equations

The mathematical models developed above consist of two systems of algebraic and nonlinear equations. The mathematical expressions describing the thermo-physical properties of sea water, steam, condensate, and brine solutions are the main contributors to the complexity and non-linearity of the equations.

In this work, we consider performance calculation for the MSF-BR process. Thus, Table 1, given by Helal et al. [8], specifies parameters whose values must be fixed. This parameters are the make-up mass flow rate (M_f), the rejected sea water flow rate (M_{cw}), the recycle stream mass flow rate (M_R), and the steam temperature (T_s). The other parameters considered as unknowns of the system are the distillate flow rate (D_j) formed in each stage j, the flashing brine mass flow rate (B_j) leaving each stage j, the flashing brine concentration (X_{bj}) at the exit of each stage j, the flashing brine temperature (T_{bj}) at the exit of stage j, the cooling water temperature (T_{fj}) at the exit of each stage j, the steam flow rate (M_s), the distillate product

Table 1
Different specifications for the MSF-BR process flowsheet

Case N	Variable specification	Referred to as
1	M_R, M_{cw}, M_f, and T_s	Performance calculation
2	M_d, T_{b0}, M_f, and M_{cw}	Fixed product flow rate
3	M_s, T_{b0}, M_f, and M_{cw}/M_R	Fixed steam flow rate

In all cases, the feed temperature T_{cw} and concentration X_{cw} are specified.

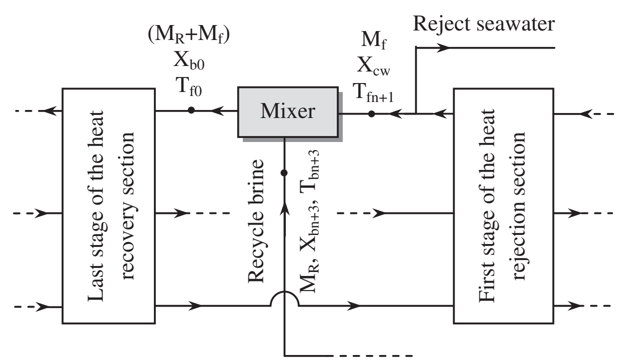

Fig. 6. Mixer.

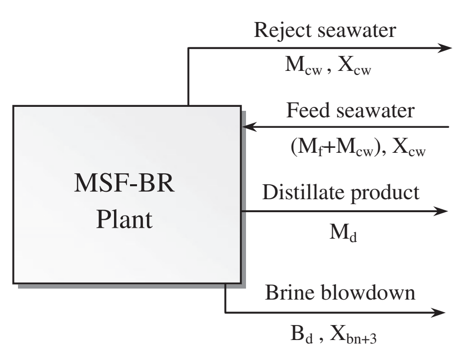

Fig. 7. Overall material balance for MSF-BR plant.

flow rate (M_d), the brine blow-down flow rate (B_d), the top brine temperature (T_{b0}), and the temperature and the salt concentration (T_{f0}, X_{b0}) of the cooling brine entering the condenser of the last stage of the heat recovery section.

In the case of the MSF-OT process, the parameters whose values were specified are: the make-up mass flow rate (M_f), the top brine temperature (T_{b0}), the feed temperature (T_{cw}), and the seawater concentration (X_{cw}). The other parameters considered as unknowns of the system are the distillate flow rate (D_j) formed in each stage j, the outlet brine mass flow rate (B_j), the outlet brine salinity (X_{bj}), the stage temperature (T_{bj}), the cooling water temperature (T_{fj}) at the exit of each stage j, and the steam flow rate (M_s).

The systems of the nonlinear algebraic equations describing the aforementioned mathematical models are written in the form $F(X) = 0$, where X the vector of the unknowns and F is the equations vector of the mathematical model. In this work, the systems were solved through an iterative procedure with using the function "fsolve" with a Solver Optimization Tool of MATLAB software. The algorithm used to solve the systems was the trust-region-reflective algorithm. To

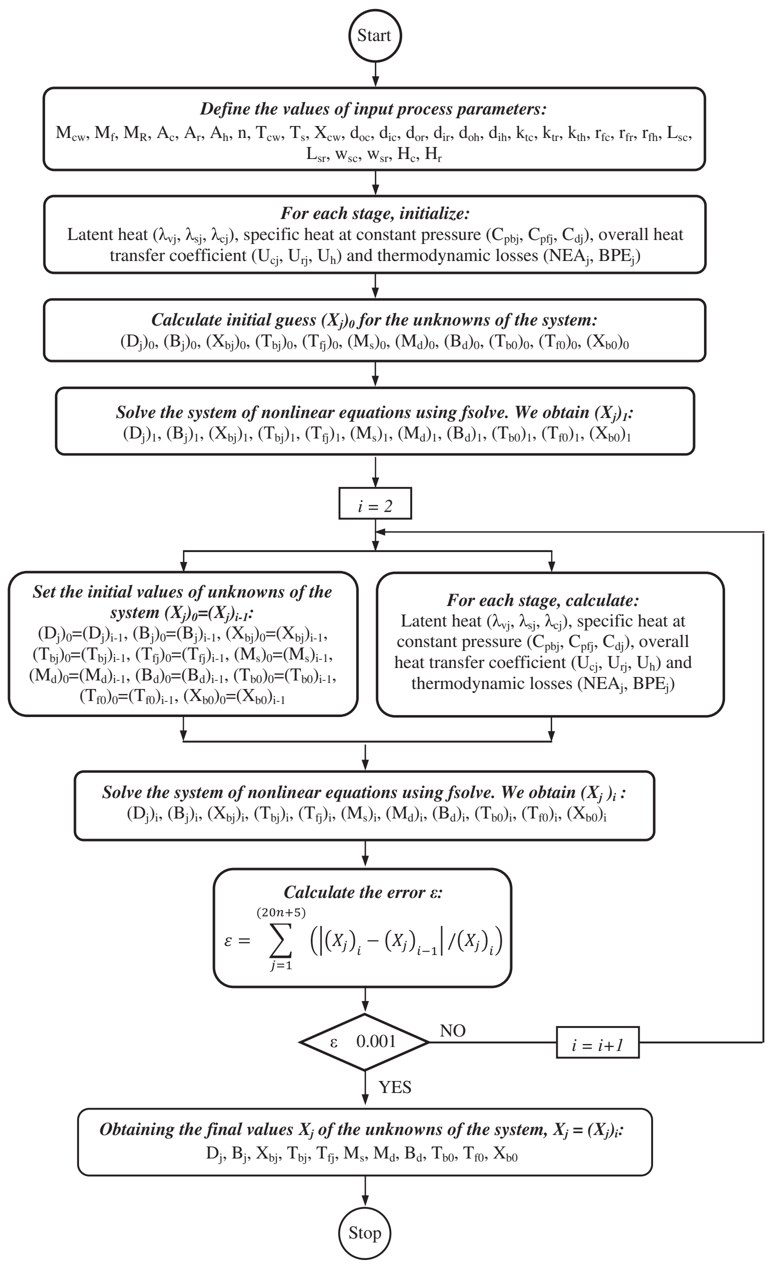

Fig. 8. Solution scheme for the MSF-BR mathematical model.

enhance convergence by predicting a good initial guesses, a simplified model given by El-Dessoukey et al. [5] was first solved. This simplified model does not need iterative solution and it is based on the following assumptions:

- Constant and equal specific heat for all liquid streams, Cp.
- Equal temperature drop per stage for the flashing brine.
- Equal temperature drop per stage for the feed brine.
- Constant and equal latent heat of vaporization in all the stages.
- Constant equal thermodynamic losses in all the stages.

The solution scheme of the system, in the case of the MSF-BR process is shown in Fig. 8. The same approach was adopted in the case of the MSF-OT process.

6. Results and discussion

The adequacy of the resolution method used in this work was tested by comparing the numerical simulation results with data reported by Rosso et al. [3] in the case of the MSF-BR process, and with field data for existing plant, reported by Al-Fulaij et al. [2] in the case of the MSF-OT process.

The MSF-BR configuration considered in this work includes 13 stages in the heat recovery section and 3 stages in the heat rejection section. The results obtained by Rosso et al. [3] and this work are based on the following input data:

Table 2
Parameters used in simulation of MSF-OT system

Parameter	Value
Number of stages (n)	21
Stage width (Wst), m	17.66
Stage length (Lst) m	3.150
Stage height (Hst), m	4.521
Number of condenser tubes (Nt)	1,410
Condenser tubes outer diameter (ODt), m	0.0445
Condenser tubes inner diameter (IDt), m	0.04197
Brine level set point in the last stage (Hst), m	0.668
Top brine temperature (TBT), ℃	91
Intake sea water flow rate (M_f), kg/s	4,027
Intake sea water salinity (Ccw), ppm	40,000
Intake sea water temperature (Tcw), ℃	37.7
Steam temperature (Tstm), ℃	111

- The condenser tubes of the heat recovery section have an outside diameter (d_{co}) of 24.4 mm, inside diameter (d_{ci}) of 22 mm, and fouling inside factor (r_c) of 1.4×10^{-4} (h m^2 K)/kcal. The material of the tubes is (Cu/Ni 90/10).
- The condenser tubes of the heat rejection section have an outside diameter (d_{ro}) of 25.4 mm, inside diameter (d_{ri}) of 23.9 mm, and fouling inside factor (r_r) of 2.33×10^{-5} (h m^2 K)/kcal. The material of the tubes is (Cu/Ni 90/10).
- The brine heater tubes have an outside diameter (d_{ho}) of 24.4 mm, inside diameter (d_{hi}) of 22 mm, and fouling inside factor (r_h) of 1.86x10^{-4} (h m^2 K)/kcal. The material of the tubes is (Cu/Ni 70/30).
- The heat transfer area (A_c) of each stage of the heat recovery section is equal to 3,995 m^2.
- The heat transfer area (A_r) of each stage of the heat rejection section is equal to 3,530 m^2.
- The heat transfer area (A_h) of the brine heater is equal to 3,530 m^2.
- Each stage of the heat recovery section has a length (L_c) of 12.2 m, a width (w_c) of 12.2 m, and a brine pool height (H_c) of 0.457 m.

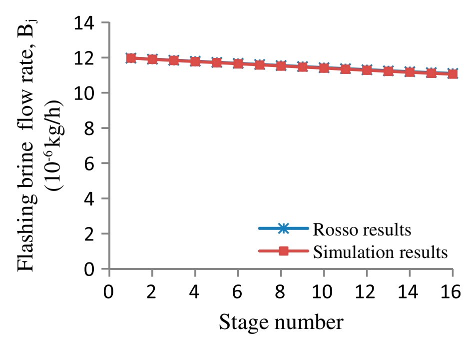

Fig. 9. Comparison of calculated brine mass flow rate and data given by Rosso et al.

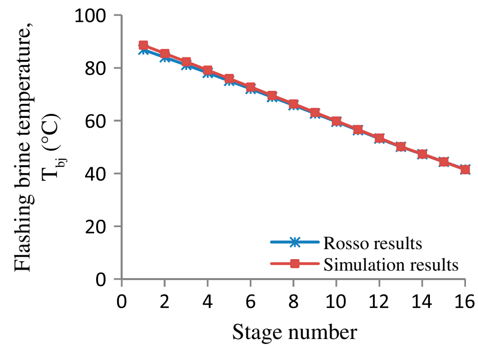

Fig. 10. Comparison of calculated temperature of flashing brine and data given by Rosso et al.

- Each stage of the heat rejection section has a length (L_r) of 10.7 m, a width (w_r) of 10.7 m, and a brine pool height (H_r) of 0.457 m.
- The temperature (T_{cw}) and salt concentration (X_{cw}) of the feed water are equal to 35°C and 57 (% w), respectively.
- Temperature (T_s) of motive steam is equal to 97°C.
- The sea water mass flow rate ($M_f + M_{cw}$) is equal to 11.31×10^6 kg/h.

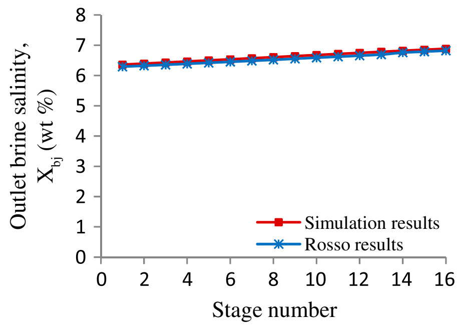

Fig. 11. Comparison of calculated outlet brine salinity and data given by Rosso et al.

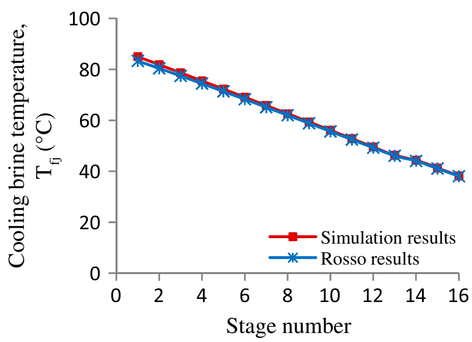

Fig. 12. Comparison of calculated temperature of brine flowing in the brine preheaters and data given by Rosso et al.

Table 3
Maximum difference between simulation results and Rosso et al.'s data

Parameter	Maximum difference (%)
Brine mass flow rate (B_j)	0.36
Salinity in the flashing brine (X_{bj})	1.35
Temperature of cooling brine leaving stage j (T_{fj})	1.89
Temperature of flashing brine leaving stage j (T_{bj})	1.84
Steam mass flow rate (M_s)	3.31
Top brine temperature (T_{b0})	2.08

- The rejected sea water mass flow rate (M_{cw}) is equal to 5.62×10^6 kg/h.
- The recycle stream mass flow rate (M_R) is equal to 6.35×10^6 kg/h.

The parameters used in the simulation of the MSF-OT system are shown in Table 2. The configuration refers to data of real plant including 21 stages [2].

Figs. 9–12 illustrate the comparison between the simulation results and data given by Rosso et al. [3] in the case of the MSF-BR process. As shown in the Fig-

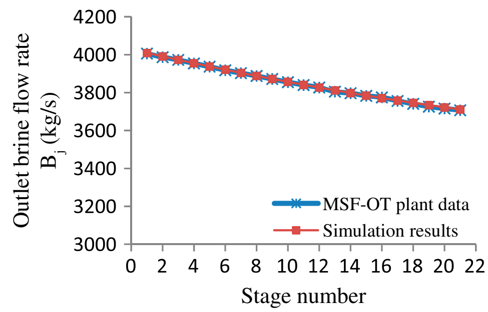

Fig. 13. Comparison of calculated brine mass flow rate and MSF-OT plant data.

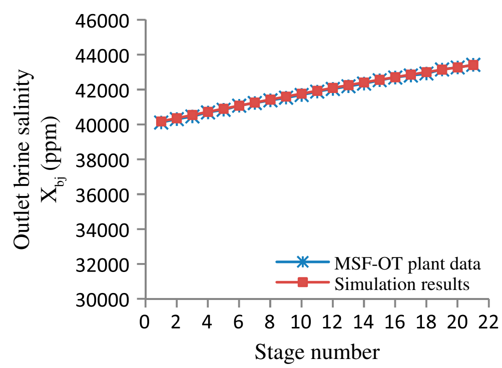

Fig. 14. Comparison of calculated outlet brine salinity and MSF-OT plant data.

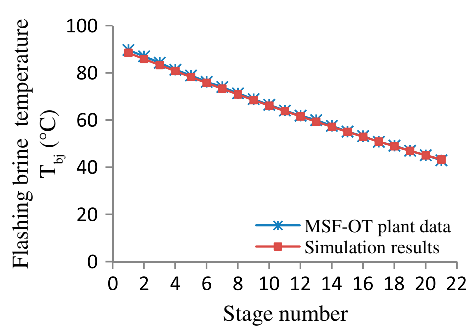

Fig. 15. Comparison of calculated temperature of flashing brine and MSF-OT plant data.

ures, there is a good agreement between the two results. Table 3. shows the maximum difference found between the two results. The slight differences are due to the use of different correlations for thermal and physical properties of various fluids.

The adequacy of the resolution algorithm in the case of the MSF-OT process was tested by comparing the simulation results with real plant data from Doha, Kuwait [2]. The comparison includes variation in the flow rate (B_j), salinity (X_{bj}), and the temperature profiles (T_{bj}) of the brine stream across the stages. As shown in Figs. 13–15, there is excellent agreement between the real and calculated data. Indeed, the relative error did not exceed 0.21% for the brine flow rate, 0.2% for the brine salinity, and 1.3% for the stage temperature.

7. Conclusions

This study presents an algorithm for solving the large system of algebraic and non-linear equations describing the steady-state model of two MSF plant configurations frequently used in the desalination industry: the MSF-BR and the MSF-OT desalination processes. The systems of equations were solved through an iterative procedure by using the function fsolve of MATLAB software. The proposed algorithm was validated by using data from previous simulation results that appeared in the literature as well as data obtained from a real MSF plant in operation. The validation results showed good agreement between the two results since the difference found did not exceed 3.31% in the case of a 16-stage MSF-BR plant and 1.3% in the case of a 21-stage MSF-OT plant.

Symbols

A — heat transfer area, m^2
B_d — blow-down mass flow rate, kg/s
B — flashing brine mass flow rate leaving stage j, kg/s
BPE — boiling point elevation, ℃
Cp — specific heat at constant pressure, kJ/kg K
C_1 — correction factor for the number of tubes in vertical direction
D — distillate formed in each flashing stage, kg/s
d_i — inner tube diameter, m
d_o — outer tube diameter, m
H — height, m
h_i — internal heat transfer coefficient, kW/m^2 ℃
h_o — external heat transfer coefficient, kW/m^2 ℃
k — thermal conductivity, kW/m ℃
L — length, m
LMTD — logarithmic mean temperature difference, ℃
M — mass flow rate, kg/s
n — number of stages of the heat recovery section
N — number of tubes in vertical direction in the tube bundle,
NEA — nonequilibrium allowance, ℃
Pr — Prandtl number
PR — thermal performance ratio
Re — Reynolds number
r_{fi} — thermal resistance of the scale on the inside of the tubes, m^2K/W
r_{fo} — thermal resistance of the scale on the outer surface of the tubes, m^2K/W
T — temperature, ℃
T_{b0} — top brine temperature, ℃
U — overall heat transfer coefficient, W/m^2℃K
w — width, m
X — water salinity, ppm

Greek

λ — latent heat, kJ/kg
μ — viscosity, kg/m s
ρ — density, kg/m^3

Subscripts

b — brine
c — recovery section
cw — cooling water
d — distillate product
f — feed stream
h — brine heater
j — stage index
l — liquid
n — last stage of the heat recovery section
r — rejection section
R — brine recycle
s — heating steam
t — tube
v — vapor

References

[1] M.S. Tanvir, I.M. Mujtaba, Optimisation of design and operation of MSF desalination process using MINLP technique in gPROMS, Desalination 222 (2008) 419–430.
[2] H. Al-Fulaija, A. Cipollina b, D. Bogle, H. Ettouney, Once through multistage flash desalination: gPROMS dynamic and steady state modeling, Desalin. Water Treat. 18 (2010) 46–60.
[3] M. Rosso, A. Beltmmini, M. Mazzotti, M. Morbidelli, Modeling multistage flash desalination plants, Desalination 108 (1996) 365–374.
[4] N.M. Abdel-Jabbar, H.M. Qiblawey, F.S. Mjalli, H. Ettouney, Simulation of large capacity MSF brine circulation plants, Desalination 204 (2007) 501–514.

[5] H.T. El-Dessouky, H.M. Ettouney, Fundamentals of Salt Water Desalination, Elsevier Science, Amsterdam, 2002.
[6] F.N. Alasfour, H.K. Abdulrahim, Rigorous steady state modeling of MSF-BR desalination system, Desalin. Water Treat. 1 (2009) 259–276.
[7] H. El-Dessouky, S. Bingulac, Solving equations simulating the steady-state behavior of the multi-stage flash desalination process, Desalination 107 (1996) 171–193.
[8] A.M. Helal, M.S. Medani, M.A. Solimani, J.R. Flowers, A tridiagonal matrix model for multistage flash desalination plants, Comput. Chem. Eng. 10 (1986) 327–341.
[9] M.A. Soliman, A mathematical model for MSF multi-stage flash desalination plants, J. Eng. Sci. Univ. Riyadh 7(2) (1981) 143–150.
[10] M.A. Darwish, Thermal analysis of multi stage flash desalination systems, Desalination 85 (1991) 59–79.
[11] H.T. El-Dessouky, I. Alatiqi, H.M. Ettouney, Process synthesis: The multi-stage flash desalination system, Desalination 115 (1998) 155–179.
[12] A. Cipollina, G. Micale, L. Rizzuti, Seawater Desalination, Conventional and Renewable Energy Process, Springer-Verlag, Berlin–Heidelberg, 2009.